Renewable Energy 67 (2014) 242–251

Contents lists available at ScienceDirect

Renewable Energy

journal homepage: www.elsevier.com/locate/renene

Performance and safety of rooftop wind turbines: Use of CFD to gain insight into inflow conditions

Amir Bashirzadeh Tabrizi [a,*], Jonathan Whale [a], Thomas Lyons [b], Tania Urmee [a]

[a] Physics and Energy Studies, School of Engineering and Information Technology, Murdoch University, 90 South Street, Murdoch, Perth, WA 6150, Australia
[b] Environmental Science, School of Veterinary and Life Sciences, Murdoch University, Perth, WA 6150, Australia

ARTICLE INFO

Article history:
Received 10 October 2013
Accepted 14 November 2013
Available online 8 December 2013

Keywords:
Small wind turbines
Built environment
CFD
Wind atlas software

ABSTRACT

The installation of small and medium-size wind turbines on the rooftops of high buildings has been often suggested by architects and project developers as a potential solution for achieving sustainable energy in building design. In such locations, however, because of the presence of buildings and other adjacent obstructions, wind is normally turbulent, unstable and weak, in terms of direction and speed. The use of wind turbines in the built environment poses challenges to overcome, including energy yield reduction due to lower mean wind speeds in urban areas, and environmental impacts because of their close vicinity to people and property.

There is a need to understand the inflow wind conditions for a small wind turbine in the built-environment. A resource assessment of the potential wind turbine site in the built environment can determine the wind characteristics including zones of wind acceleration, recirculation, blocking and channelling. This knowledge is crucial for input into the design process of a small wind turbine to accurately predict blade fatigue loads and ensure that it operates safely, and performs optimally in the environment.

Computational Fluid Dynamics (CFD) is a useful method to model wind flows in order to perform a resource assessment for the application of small wind turbines in a manner that requires less time and investment than a measurement campaign. This paper presents the results of research using a CFD code to model wind flows over the roof of a building and assesses the possibility of combining a CFD package with wind atlas software to form a wind energy resource assessment tool for the application of small wind turbines on the roof of a building. Experimentation with the model shows that the results are particularly sensitive to building height and shape, roof shape, wind direction, and turbine installation height and location. The results will be used to help develop a recommended practice of wind resource assessment in the built environment, in an international collaborative effort via the International Energy Agency Task 27.

© 2013 Elsevier Ltd. All rights reserved.

1. Introduction

A growing public awareness of the rising level of greenhouse gas emissions, the need to tackle fuel security and achieve reductions in emissions, has resulted in significant efforts to adopt renewable energy technologies in suburban environments [1–3]. These efforts aim to reduce the energetic demand of urban centres, and small-size renewable energy systems represent an interesting solution for sustainable (and reduced) energy in new building design [4]. The integration of wind turbines into the built environment poses challenges due to the low energy yield resulting from low mean wind speeds in urban areas as well as environmental impacts [5]. There have been some very public failures of small wind turbines in the built environment, notably in situations where the turbines have been mounted on top of the buildings [6–8]. Despite these problems, local governments and businesses continue to install SWTs on their rooftops as a dynamic, visible sign of support for renewable energy. It is thus vital to make the installations safe and to optimise performance to avoid them becoming bad advertisements for wind energy and renewable energy in general. To accomplish this, it is important to know the inflow wind conditions for SWTs in urban areas.

Due to the existence of obstacles with different shapes, high roughness lengths of the terrain and obstacles' interference to wind flow, wind conditions in urban locations are very complex and the

* Corresponding author. Tel.: +61 893606713.
E-mail addresses: a.btabrizi@murdoch.edu.au, bashirzadeh@hotmail.com (A.B. Tabrizi).

0960-1481/$ – see front matter © 2013 Elsevier Ltd. All rights reserved.
http://dx.doi.org/10.1016/j.renene.2013.11.033

adaptability of wind turbines to this environment is not yet tested both in terms of real power production and of structural compatibility with the buildings. As a result, the wind profile in urban locations is quite different from the classical log-law based profile used in open terrain [9]. At the open terrain sites of large wind turbines, performing comprehensive wind resource assessments yields knowledge about the characteristics of the lower part of the atmosphere as well as parameters like annual and seasonal average wind speed and turbulence characteristics. Turbulence is an important parameter to factor into wind turbine design as it causes cyclic loading on the blades and can lead to blade fatigue. In comparison, small-scale wind turbines are often located in more complex environments where the turbulence levels are higher and wind speeds are lower [10]. In understanding the inflow to a small wind turbine in the built-environment a resource assessment of the potential wind site can be used to determine the wind characteristics, including turbulence levels that the small wind turbine will have to experience. Recent research by the International Energy Agency (IEA) Wind RD&D Task 27, a vehicle for SWT research, has indicated that the turbulence design thresholds in the current international standard for SWTs, IEC61400-2 (ed. 3) are too low for SWTs in urban wind sites, and a better characterisation of turbulence is required for these kind of highly turbulent sites [11].

Wind resource assessments for utility-scale wind projects typically involve lengthy and costly measurement campaigns. For small wind turbines application particularly rooftop applications, conventional site assessment methods are not always useful due to the small-scale of the projects. Firstly, compared to utility-scale or community-scale wind projects, small-scale urban rooftop projects do not typically have access to large amounts of fiscal resources for the resource assessment phase of a project and thus investment in measurement equipment usually is limited. In addition, for urban environments, the traditional methods for wind energy site assessment are technically limited; the complex geometry can result to the situation where the resource varies substantially within a small area, thus a meteorological mast installed at a single location may not be a sufficiently good indicator of the overall resource within a complex environment. Further, remote sensing technologies such as LiDAR are typically designed to work at 40 m or above and many small-scale urban rooftop projects are designed for deployment at lower heights. Computational Fluid Dynamics (CFD) techniques can be a reliable alternative for less expensive and faster resource assessments of rooftop small wind turbine applications, and additionally provide physical insight to the governing flow mechanisms. Already, for modelling wind flows over complex rural terrains, modern CFD tools have proved essential [12].

Ledo et al. present a numerical study of wind flow above the roof in three suburban landscapes specified by houses with three different roof shapes; pitched, pyramidal and flat. They used a CFD technique to simulate the wind flow in such environments and to find the optimum turbine mounting locations. Their results show that the wind flow characteristics are strongly dependent on the shape of the roofs, with turbines mounted on flat roofs likely to generate higher and more reliable power for the same turbine hub elevation than the other roof profiles [2]. Heath, Walshe and Watson used CFD to model the flow characteristics within an urban area over an array of pitched-roof houses. They studied mean wind speeds at potential turbine mounting points and identified optimum mounting points for different prevailing wind directions. In addition they proposed a methodology for estimating the energy yield of a building-mounted turbine from simple information such as wind atlas wind speed data and building density. The results of the research show that the energy yield is very low when the turbine is installed below rooftop height [13]. Kalmikov and his team at Massachusetts Institute of Technology (MIT) used CFD simulations to assess the wind energy potential on the MIT campus in Cambridge, MA. They incorporated wind measurements and observations from some local reference sites into the CFD model in order to estimate the local long-term climatology. Comparisons of measurements and simulated results provided validation of the modelling for mean wind speed, wind power density and wind variability, parameterised by a Weibull distribution. Their work resulted in a better understanding of the micro-climate of the wind resource on the MIT campus and addressed the optimal siting of a small turbine on campus [12]. Finally, it must be noted that CFD has been used by several researchers to evaluate the performance of H-Darrieus small wind turbines on rooftops [9,14,15].

The ANSYS CFX 14 CFD software package [16] is used in this research to model wind flows over a building and is validated using secondary data from the CEDVAL wind tunnel datasets from Hamburg University. The CFD model of Bunning Group Ltd's warehouse at Port Kennedy in Western Australia was developed using the wind atlas software WAsP [17] to predict the wind velocities at the domain inlet. The research is novel as the CFD simulations are carried out on a building (the Bunnings warehouse) where there is an existing measurement system in place, allowing direct comparison between measurements and the model output. The research is also timely as it forms part of the current IEA Task 27 program of work that is developing a Recommended Practice for micro-siting SWTs in the built environment [18]. The long-term research plan is to use this Recommended Practice in order to update the design classifications in the current IEC61400-2 standard to include a class for SWTs intended for use in highly turbulent sites such as in the built environment.

2. Aim and objectives

The aim of this study is to gain an insight into the wind conditions for a SWT in the highly turbulent setting of the rooftop of a large building in order to provide guidance in micro-siting wind turbines. The specific objectives to achieve this aim are:

(1) Assess the combination of the CFD package CFX with the wind atlas software WAsP as a wind energy resource assessment tool for the application of small rooftop wind turbines in built environment.
(2) To use the combination of CFX and WAsP to investigate the effects of complex urban topography on the local micrometeorological features of the wind flow via identification of zones of wind acceleration, recirculation and blockage. An understanding of the location and extent of these zones on the rooftop is important in the installation of a small wind turbine to maximise energy production and protect the machine from excessive loading due to gusts

In terms of scope, this paper does not cover the investigation of available wind power or turbulence kinetic energy of the wind flows on the rooftop.

3. Methodology

To assess the combination of a CFD package with wind atlas software as a wind energy resource assessment tool for the built environment, a CFD model of Bunnings warehouse was created by means of the ANSYS CFX 14 software, and buildings around the warehouse, up to 200 m radius, were added to the model domain. The built-up area surrounding the warehouse is shown in Fig. 1. To predict the wind velocity at the inlet of the CFD domain, the wind atlas software WAsP was used; raw data from the Kwinana Industries Council (KIC) meteorological station located on Alcoa RDA

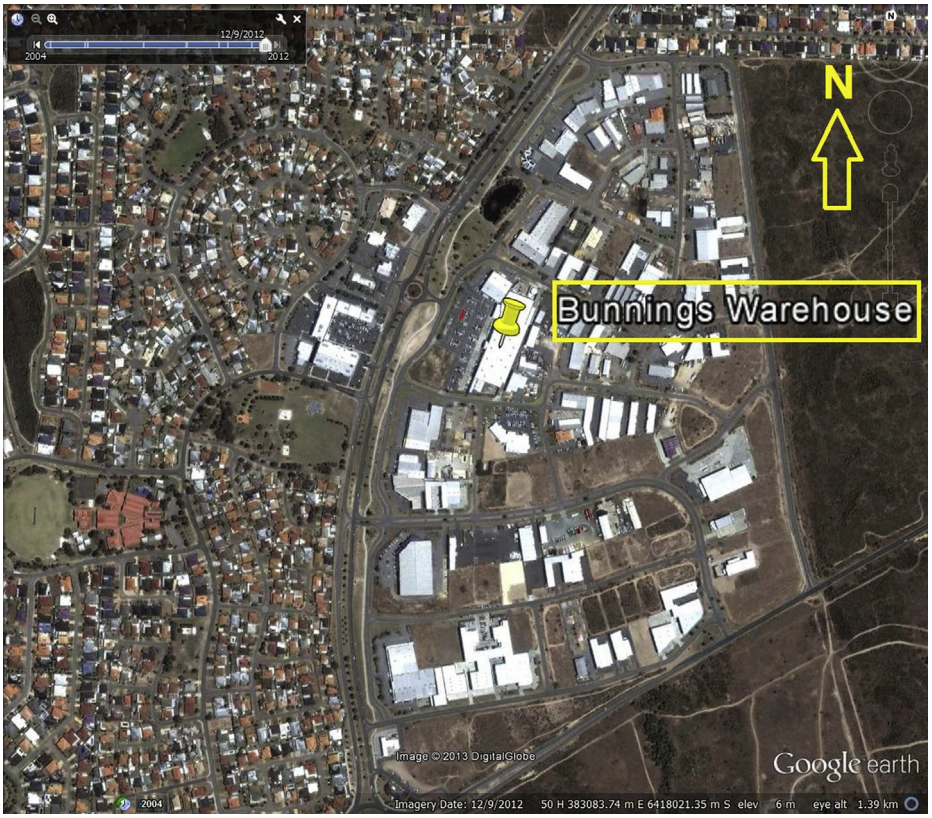

Fig. 1. The built-up area surrounding the Bunnings warehouse in Port-Kennedy, Western Australia.

Fig. 2. The location of Alcoa RDA Lake meteorological station compared to the location of the Bunnings warehouse in Port-Kennedy, Western Australia.

Lake A, recorded between 12/08/2011 and 24/01/2012 were used as wind observations in WAsP. Fig. 2 shows the location of the meteorological station compared to the location of the Bunnings warehouse. WAsP was used to generate a regional wind atlas for eight wind direction sectors N, NE, E, SE, S, SW and W at 200 m above the ground. At 200 m above the ground the wind characteristic for each sector is not affected by surface structures, and was used to predict the site-independent vertical wind profile for the region. This profile was then used as the inlet velocity profile at the outer boundary of the CFD model domain and the model was run for each sector to find the mean wind velocities on the roof of the warehouse. To allow for comparison the CFD results were extracted for the same period as the KIC measurements and ultrasonic measurements of wind flow on the roof of the Bunnings warehouse (12/08/2011 to 24/01/2012). ANSYS CFX assumes neutral atmospheric stability and thus the CFD results have been compared with neutrally stable measured wind data as well as with the whole set of measured data for the period to check the accuracy of using the combination of CFD and wind atlas software for rooftop wind resource assessment. To isolate the neutrally stable data, the wind measurements above the Bunnings rooftop were filtered by application of Golder's curve of the Pasquill stability classes as functions of Monin–Obukhov length, and roughness length [19]. The European Wind Atlas was consulted and the aerodynamic roughness of area around the Bunnings warehouse was estimated to be 50 cm [20].

3.1. Site and measurement campaign

The warehouse is a rectangular building, with its long-axis oriented NNE-SSW, a façade wall around the edge of the roof with a top that is 8.4 m a.g.l, and a very low pitched roof (almost flat). The building is approximately 5 km from the coast (Indian Ocean) with the prevailing winds from the south-west. The warehouse is situated in a commercial estate but has no larger buildings or trees in the vicinity. Within a 1 km radius of the site there are mainly residential buildings to the north, commercial and industrial buildings to the east and a few buildings, low shrubs and low sand dunes to the south and west. The south-west front and the north-west side are comparatively open, though street furniture[1] and a car park exist on these sides [21].

A wind monitoring system was installed in September 2009 as part of a wind resource assessment for the installation of five small wind turbines that were later installed in March 2010. The Gill WindMaster Pro 3D ultrasonic anemometer was installed on a boom on a 5.3 m tall mast attached to the front-façade of the warehouse. The boom had a sliding collar in order to position the ultrasonic anemometer at different heights above the roof. The mast could be tilted down in order to make adjustments or to replace sensors. The data consists of 10 Hz data over a six-month period (between 12/08/2011 and 24/01/2012). Fig. 3 indicates the position of the ultrasonic anemometer on the roof.

3.2. Computational fluid dynamic model

3.2.1. Navier–Stokes equations and turbulence models

ANSYS CFX 14 developed by ANSYS, Inc., USA was used to perform the CFD simulations. Different methods such as Direct Numerical Simulation (DNS) [22], Large Eddy Simulation (LES) [23,24], or the Reynolds-averaged Navier–Stokes (RANS) approach with various turbulence models [25,26] have been applied in CFD simulations. The required flow detail and the available computing resources are two critical criteria for choosing the best method. Usually, it suffices to use the well-established RANS equations when only quasi-steady data is of interest, and that approach has been taken in the present study [2].

Fig. 3. Position of the ultrasonic anemometer on the roof of the Bunnings warehouse in Port-Kennedy, Western Australia.

For modelling wind flow over complex terrain, the Reynolds-averaged Navier–Stokes approach (RANS) combined with a k-epsilon $k-\varepsilon$ scheme as turbulence model, is the most common approach in wind engineering. The method provides a fair compromise between computational costs and accuracy. Reynolds decomposition is employed to the variables of the governing equations, whereby each variable is divided into a time-averaged part and a fluctuating part, $u = \overline{u} + \acute{u}$, resulting in the two following equations:

$$\rho\left(\frac{\partial \overline{u}_i}{\partial t} + \overline{u}_j\frac{\partial \overline{u}_i}{\partial x_j}\right) = -\frac{\partial \overline{P}}{\partial x_i} + \rho\overline{g}_i + \frac{\partial}{\partial x_j}\left[\mu\left(\frac{\partial \overline{u}_i}{\partial x_j} + \frac{\partial \overline{u}_j}{\partial x_i}\right)\right] - \frac{\partial}{\partial x_j}\rho\overline{\acute{u}_i\acute{u}_j} \quad (1)$$

$$\frac{\partial \overline{u}_k}{\partial x_k} = 0 \quad (2)$$

The terms $\overline{\acute{u}_i\acute{u}_j}$ as the Reynolds stresses and physically represent the additional stresses due to the fluctuating components of the flow. These Reynolds stresses have been modelled according to a 'Boussinesq' approximation, shown in Eq. (3), an analogy of Newton's friction law:

$$\tau_{ij} = -\overline{\rho\acute{u}_i\acute{u}_j} = \mu_t\left(\frac{\partial u_i}{\partial x_i} + \frac{\partial u_j}{\partial x_i}\right) + \frac{2}{3}\rho k\delta_{ij} \quad (3)$$

where μ_t is the turbulent viscosity and $k = 1/2\overline{\acute{u}_i\acute{u}_j}$ is the turbulent kinetic energy (TKE). The 'standard' k–epsilon $(k-\varepsilon)$ model, based on a two-equation turbulent energy scheme provides reasonable results in approximately neutral atmospheric conditions, and provides an acceptable estimate of the turbulence intensity through the turbulent kinetic energy term [27].In this study, there was improved convergence of the CFX results using the Shear Stress Transport (SST) scheme. The SST scheme is a hybrid of two-equation models that combines the advantages of both k–epsilon $(k-\varepsilon)$ and k-omega $(k-\omega)$ models. The SST $k-\omega$ equations are:

[1] Objects and pieces of equipment installed on streets and roads for various purposes.

$$\frac{\partial \rho k}{\partial t}+\frac{\partial}{\partial x_j}(\rho U_j k) = \frac{\partial}{\partial x_j}\left[\left(\mu+\frac{\mu_t}{\sigma_{k3}}\right)\frac{\partial k}{\partial x_j}\right]+P_k-\beta'\rho k\omega+P_{kb} \quad (4)$$

$$\frac{\partial \rho \omega}{\partial t}+\frac{\partial \rho \omega}{\partial x_j}(\rho U_j k) = \frac{\partial}{\partial x_j}\left[\left(\mu+\frac{\mu_t}{\sigma_{\omega 3}}\right)\frac{\partial \omega}{\partial x_j}\right]+(1-F_1)2\rho\frac{1}{\omega\sigma_{\omega 2}}\frac{\partial k}{\partial x_j}\frac{\partial \omega}{\partial x_j} - \alpha_3\frac{\omega}{k}P_k-\beta_3\rho\omega^2+P_{\omega b} \quad (5)$$

where F_1 is a blending function, P_k is turbulence production due to viscous forces [kg/ms^3], P_{kb} and P_{wb} are buoyancy production terms [kg/ms^3], α is wind direction [°], β is a sheltering effect factor,$\sigma_{\omega 2}$ and $\sigma_{\omega 3}$ are constants in the SST $k-\omega$ is turbulence model and ω is the turbulent energy dissipation rate [1/s]. The SST $k-\omega$ model incorporates transport effects in the formulation of the eddy-viscosity terms and thus pays more attention to the transport of turbulence kinetic energy, and predicts the starting and the size of the separation of flow under adverse pressure gradients more accurately than the standard $(k-\varepsilon)$ model. This leads to improvement of prediction of the flow separation, which is important in the present study [2].

3.2.2. Inlet wind profile

The velocity profile at the inlet boundary of the simulation domain must be accurately modelled to provide valid results of wind simulation in the built environment. The roughness of the ground affects the profile of wind velocity, u, and therefore is necessary to be part of velocity profile simulation. The following equation is used to model the wind profile at the inlet of CFD domain:

$$u = \frac{u_*}{k}\ln\left(\frac{y+z_0}{z_0}\right) \quad (6)$$

where z_0 is the ground roughness of the area, u_* is the friction velocity, and k is von Karman's constant and is equal to 0.4. Since all the buildings within a radius of 200 m around the target building have already been simulated in the CFD model, the ground roughness is set to 2 cm for all wind sector simulations. For each simulated sector, the mean wind speed at 200 m above the ground (the output of the WAsP simulations) was used to find the friction velocity for the CFD simulation. Table 1 shows the results of the WAsP simulations in terms of mean wind speed for each sector.

3.2.3. Computational mesh

An unstructured tetrahedral mesh was used with five inflation layers of 25 mm total thickness on the ground, roofs and walls of all buildings. A cross-section of the mesh for the North wind sector is shown in Fig. 4. The final mesh statistics in the modelling of wind flow from eight wind sectors are shown in Table 2. The domain of the CFX models for all simulated wind sectors was set up as a rectangular domain surrounding the urban grid.

Table 1
WAsP output: sector-wise mean wind speeds at 200 m.

Wind sector	Mean wind speed (m/s)
North	6.36
North East	5.33
East	8.01
South East	7.57
South	8.53
South West	8.36
West	6.19
North West	6.18

3.2.4. Boundary domain and boundary conditions

For all wind sectors, the simulated buildings were placed in a rectangular domain of height equal to 200 m and the lateral boundaries of the computational domain were placed at a distance of $5H_{max}$ away from the closest part of the built area at each side, where H_{max} is the height of the highest simulated building in the region of interest. A distance of $8H_{max}$ between the inflow boundary and the built area was applied as the longitudinal extension of the domain in front of the simulated region, and $15H_{max}$ behind the built area was employed to allow for flow re-development.

The turbulence level at the inlet boundary was adjusted to 5% as suggested by CFX guidelines [16]. The downstream boundary was specified as an outlet with zero relative pressure and zero turbulence intensity gradients. Symmetric boundary conditions were employed for the side faces and top of the domain in all wind sectors. Solid boundaries including the ground of the domain and roofs and walls of the buildings have been set as no-slip walls with the CFX wall-function approach used to model flow near these surfaces [28]. An automatic near-wall treatment method was deployed by CFX to treat the wall effects. The near-wall treatment method accounts for the rapid variation of flow variables that occur within the boundary layer region as well as viscous effects at the wall. This treatment provided a smooth shift from low-Reynolds number formulation to wall function formulation.

4. Test case: flow around a rectangular obstacle

A test case was performed to model the flow around a rectangular structure to assess the accuracy of CFX in simulating flow around obstacles. The simulation results were then compared with the well-known CEDVAL wind tunnel datasets from Hamburg University [29]. All data sets within the CEDVAL database have high quality and complete documentation of boundary conditions and application of quality assurance checks during measurements The rectangular structure from the CEDVAL wind tunnel tests has dimensions of 125 mm height, 100 mm width and 150 mm length. The Reynolds number of the model test is 37,250 and the roughness length of the model is 0.007 m. The friction velocity and the offset height of model boundary layer is 0.377 m/s and 0 m respectively.

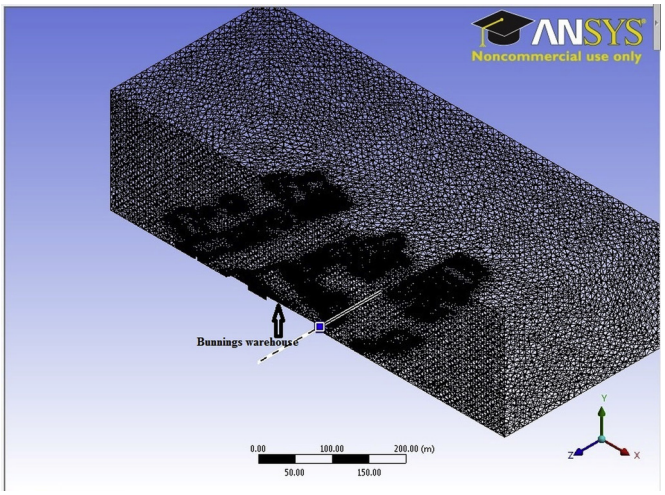

Fig. 4. Cross-section of the mesh for the North wind sector modelling of the Bunnings warehouse in Port-Kennedy, Western Australia.

Table 2
Final mesh statistics for all simulated wind sectors.

Wind sector	Number of elements	Number of nodes
North	2121517	664904
North East	2475462	806925
East	2219394	707034
South East	1885504	594546
South	2511951	799133
South West	2104457	649320
West	2274320	719881
North West	1885504	594564

The values of longitudinal and vertical wind components for 603 points in the vertical plane and the values of longitudinal and lateral wind components for 660 points in the horizontal plane have been provided in the data set. The data set also includes a visualisation of flow around the structure in both horizontal and vertical planes.

The CFX simulation domain and obstacle was set up in a similar way to the configuration used in the CEDVAL data set and the rectangular obstacle was meshed using a 125 mm cell edge length with two inflation layers of 10 mm thickness near the walls. The wind flow in the CFX model was set to give a Reynolds number of 37,250 as reported in the CEDVAL data set and equation (6) was used to simulate the inlet velocity profile, setting z_0 equal to 0.007 m as the ground roughness of the model.

4.1. Test case validation

The comparison of numerical simulation results and corresponding experimental data with the aid of a metric is the core of CFX code validation. A validation metric is a mathematical operator that specifies the accuracy of the results from numerical simulation by comparing them with results from experimental test [30]. The metric should supply information on the agreement, or disagreement, between the results of numerical simulation and experimental results. General and desirable features of metrics have been formulated by Oberkampf and Barone [31].

The 'hit rate' metric is used as a metric in the present work to test the CFX accuracy in simulating flow around obstacles. This metric has been suggested in guidelines by the Association of German Engineers (VDI) [32] and has been used in many previous investigations [33–35] for validating numerical simulations. Experimental and simulation results should be available at the same positions to compute any metric, therefore the same points in the same plane as the CEDVAL data set have been generated in the simulation. Since the experimental measurement points don't typically coincide with the computational grid cell centres, interpolation of the numerical simulation results is essential. The validation metric hit rate, q, is calculated, after achieving the numerical results available at all experimental measurement positions [36,37]. In the permissible absolute difference, the uncertainty of measurement performs acts as a threshold while the relative difference becomes meaningless for experimental data approaching zero in the denominator (especially for lateral and vertical wind components that have very low normalised value) and therefore the permissible absolute error has been used in this study to calculate metric hit rate.

Table 3
Hit rate values for wind components in modelling the flow around a rectangular obstacle.

Item	Hit rate value (%)
Longitudinal wind component	73
Lateral wind component	82
Vertical wind component	79

According to VDI Guideline 3783 Part 9, 2005 [32], a hit rate of $q \geq 0.66$ for each velocity component is required to pass the validation test. This criterion was used for the hit rates based on all valid measurement positions in the CEDVAL data set. Table 3 shows the hit rate values for longitudinal, lateral and vertical components of wind speed for simulated flow around the rectangular obstacle for the purposes of testing CFX accuracy.

As Table 3 presents, the resulted hit rate value met the criteria for all three wind components and therefore the CFX modelling of flow around a rectangular obstacle appears valid. This test case study shows that the CFX provides enough accuracy to simulate the flow around the obstacle and potentially a good tool for simulating the flow in the built environment.

5. Results and discussion

Table 4 shows the CFD simulated and measured results for the magnitude of the 10-minute averaged 3D velocity vectors on the rooftop of the Bunnings warehouse over the period 12/08/2011 to 24/01/2012, for purely neutral and for varying atmospheric conditions. The percentage of error between numerical results and measured results has been presented in the table for all wind sectors.

In terms of neutrally stable atmospheric conditions, the closest agreement between simulation and measurement (2.6%) is obtained for prevailing winds from the south-west sector. There is also reasonable agreement for north, south-east and west sectors, as the error between simulation and measurement is less than 10%. The poorest agreement comes from the south, north-east and north-west sectors where errors are more than 25%. The average error between simulation and measurement for all eight wind sectors is 16.1 percent. Table 4 shows a general trend across wind sectors of increasing error between simulated results and measured

Table 4
CFD simulation versus measurements of 10-minute averaged wind speeds on the rooftop of the Bunnings warehouse.

Wind sector	CFD (m/s)	Measurement neutrally stable condition (m/s)	Error (%)	No. of measured data – neutrally stable data	Measurement whole dataset (m/s)	Error (%)	No. of measured data – whole dataset
N	4.3429	4.1347	5.0	76	3.3665	29.0	182
NE	2.4954	3.5827	−30.3	250	2.8780	−13.3	1068
E	3.7422	4.5182	−17.2	520	3.8198	−2.0	1861
SE	4.5900	4.2027	9.2	451	3.4711	32.2	1697
S	5.6381	4.5000	25.3	718	3.9313	43.4	1430
SW	5.8489	5.6998	2.6	955	5.3290	9.8	1752
W	4.6927	5.2132	−10.0	345	4.7421	−1.0	862
NW	4.3355	6.1329	−29.3	229	5.5433	−21.8	674

data as the number of measured data points in a wind sector reduces to e.g. less than 1000. The large error in the north-east sector, despite the relatively high number of measured data in this sector, may be due to the fact that the five small wind turbines installed on the edge of the Bunnings warehouse roof were simulated as simply five masts in CFX, and in reality have more effect on the wind in north-east sector. The discrepancy in results for north-west sector is likely to be due to a combination of lack of measured data from that sector together with the effect of some high light towers around the building that clearly cause some disturbance in the north-west sector not catered for in the CFD model. Finally, the small distance between the façade and the measurement mast for cases when the wind comes from the south may be the cause of the poor agreement for the south sector simulation as there is not enough distance between the façade and the mast in the CFD model to simulate flow re-development after the wind flow passes the façade before encountering the measurement mast.

In terms of comparison of the simulations with the whole set of measured data (across all atmospheric stability classes) the minimum error is 1.0 percent for the west wind sector and the numerical results for the north-east, south-west and east sectors are reasonable with errors less than approximately 15%. For the north, south, north-west and south-east sectors, however, the simulation results are poor with errors around 21% or greater. The average error for all wind sectors is 19.1 percent. As the values in Table 4 show, the combination of WAsP and CFX predicts neutrally stable flows over the building reasonably well, however the results are not good enough to predict the flow across the whole range of atmospheric conditions; Table 5 provides meteorological conditions defining Pasquill turbulence types [38]. Table 5 clearly shows that for most cases at wind speeds greater than 4 m/s the atmospheric condition is neutral. Since the wind speeds in the operating range of many small wind turbines would be above 4 m/s and thus dominated by neutrally stable atmospheric conditions, the findings of this paper suggest that the assumption of neutral stability in the CFX software does not place a significant limitation in the application of the software, and the CFX/WAsP approach is a promising tool to predict wind speeds above the rooftops of buildings in the built environment. Some caution, however, needs to be used especially in the case of wind turbines with cut-in wind speeds below 4 m/s and in the case of strong-moderate daytime insolation levels.

Figs. 5–7 show some examples of output from CFX for the case of winds from the south-west sector, which is the prevailing wind direction at the site of the Bunnings warehouse. Fig. 5a and b show contour plots of the magnitude of wind velocity on the long west-facing roof edge, where the turbines and ultrasonic anemometer are installed, and on the middle of the roof in the longitudinal sense of the Bunnings warehouse building, respectively. Contour plots of the wind velocity vertical component for the long west-facing roof edge and on the middle of the roof in the longitudinal sense of the building have been presented in Fig. 6a and b, respectively, and Fig. 7a and b show vector plots of wind velocity on the long west-facing edge and on the middle of the roof in the longitudinal sense of the building. Comparison of Fig. 5a and b show that the magnitude of the wind velocity is slightly greater on the edge than in the middle of the roof. More marked is the difference in vertical wind components at the edge of the building and the middle; the vertical components are much greater on the edge of the roof (Figs. 6a and 7a) and this is clearly visible in the contour plots of vertical wind components (Fig. 6a and b) as well as the vector plots of wind velocity (Fig. 7a and b). These figures have an important consequence for small horizontal-axis wind turbines (HAWTs) in terms of efficiency since they are not designed to harness the vertical component of flow. Further, the vertical component of the wind velocity can have a significant effect on a HAWT in terms of fatigue loads. Therefore, the ideal location for installation of a small wind turbine, particularly a HAWT, should be in the middle of the roof of the Bunnings warehouse where the machine is likely to experience lower fatigue loads due to vertical flow and will thus have a greater life time. Balduzzi et al. found that roofs with an inclination angle of 8° were optimal in inducing a speed-up of flow

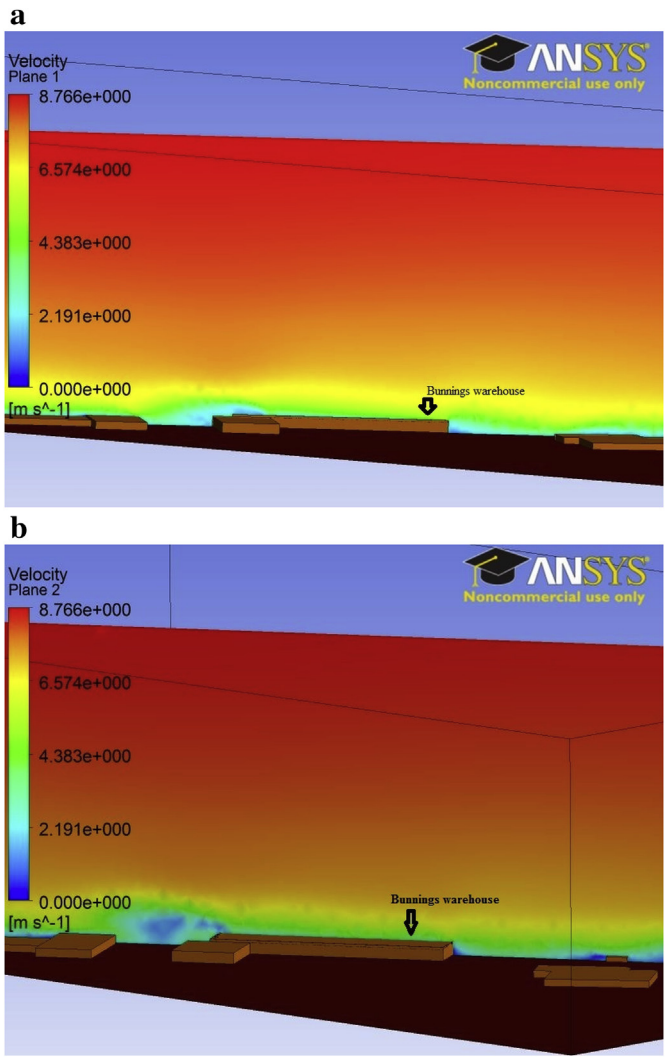

Fig. 5. a. Wind speed contours on the edge of the roof of the Bunnings warehouse for the south-west wind sector simulation. b. Wind speed contours on the middle of the roof of the Bunnings warehouse for the south-west wind sector simulation.

Table 5
Meteorological conditions defining Pasquill turbulence types [38].

Surface wind-speed (m/s)	Daytime insolation			Nighttime conditions	
	Strong	Moderate	Slight	Thin overcast or ≥4/8 low cloud	Cloudiness ≤3/8
<2	A	A–B	B	–	–
2–3	A–B	B	C	E	F
3–4	B	B–C	C	D	E
4–6	C	C-D	D	D	D
>6	C	D	D	D	D

Notes: A, extremely unstable; B, moderately unstable; C, slightly unstable; D, neutral (applicable to heavy overcast day or night); E, slightly stable; F, moderately stable; (for A–B take average of values for A and B, etc.).

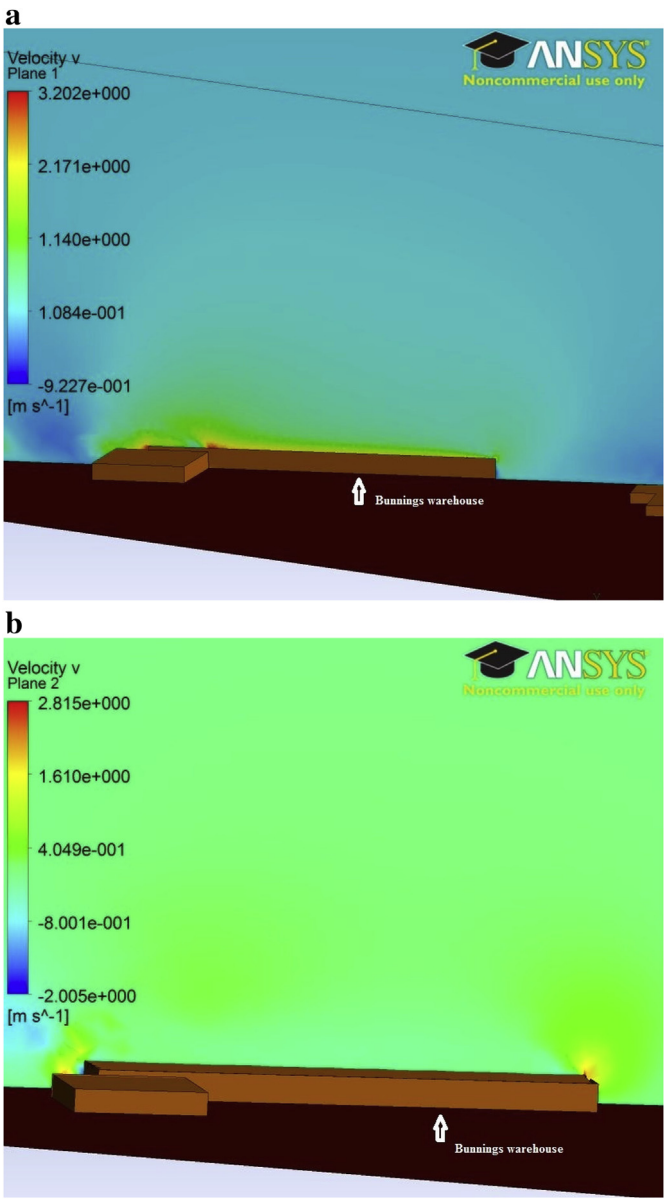

Fig. 6. a. Contours of vertical wind component on the edge of the roof of the Bunnings warehouse for the south-west wind sector simulation (Note that the vertical component is represented by v in CFX). b. Contours of vertical wind component on the middle of the roof of the Bunnings warehouse for the south-west wind sector simulation (Note that the vertical component is represented by v in CFX).

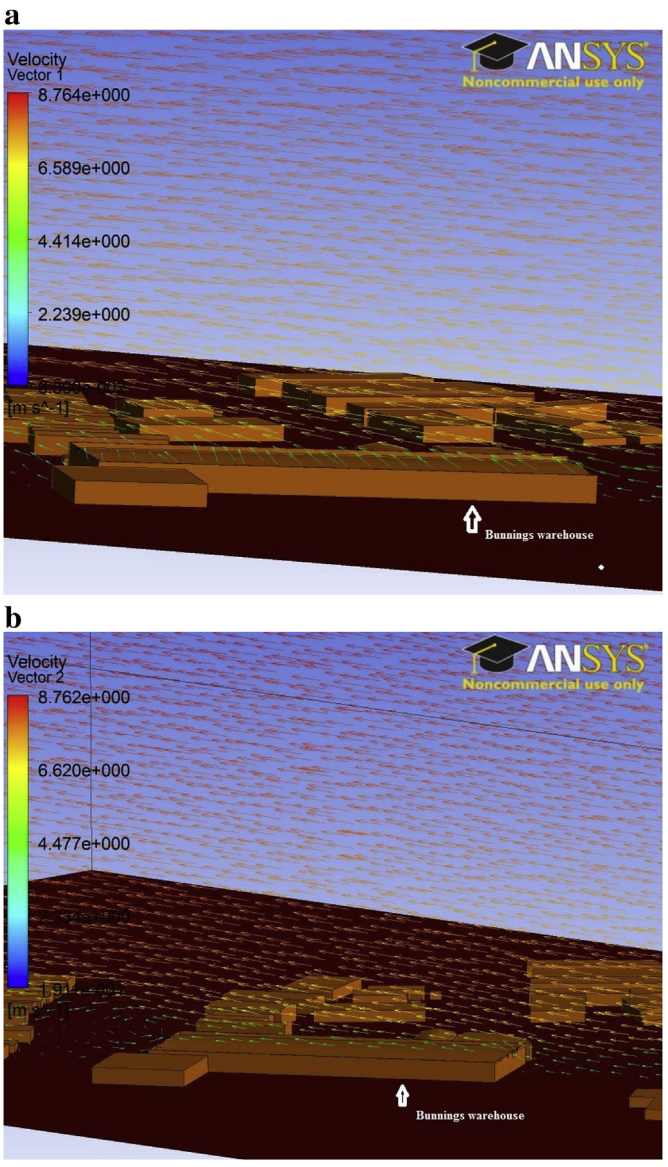

Fig. 7. a. Wind velocity vectors on the edge of the roof of the Bunnings warehouse for the south-west wind sector simulation. b. Wind velocity vectors on the middle of the roof of the Bunnings warehouse building for south-east wind sector simulation (prevailing wind direction).

over the building [9]. The sloping angle on the roof of the Bunnings warehouse is less than 8° but, as Fig. 8 suggests, the small inclination angle of the roof is effective in speeding-up the flow over the building and this is another reason for installation of small wind turbines in the middle of the roof for Bunnings warehouse building, where, if placed on a suitably tall mast, the turbines can avoid the turbulence close to the edge of the roof, and capture the increased wind speeds in the skewed flow over the building.

Figs. 5b and 7b show that on the middle of the roof, the wind is slightly channelled after passing the short south-facing edge of the building and there is a zone of wind acceleration on top of the façade at this edge as well as a blockage zone behind the façade on the south-facing edge. There is a large recirculation zone behind the short north-facing edge of the building (Fig. 7b) and this roof edge would be the worst place to install a wind turbine.

Before drawing conclusions from this research, the limitations of the study must be noted. Firstly, only a few months of measured data have been taken (August to January) covering only the spring and summer seasons in the southern hemisphere and a year long period of measured data on the rooftop would be preferable in order to consider seasonal effects. In addition, for the WAsP simulation reference data have been taken from a meteorological station 18 km away from the target building. This could be a source of error if the reference and target site do not have the same underlying regional wind climate; an assumption that has been made in using the WAsP software.

6. Conclusion

In this study, the combination of CFD package and wind atlas software was assessed as a wind resource assessment tool for a small wind turbine installation on a rooftop in the built

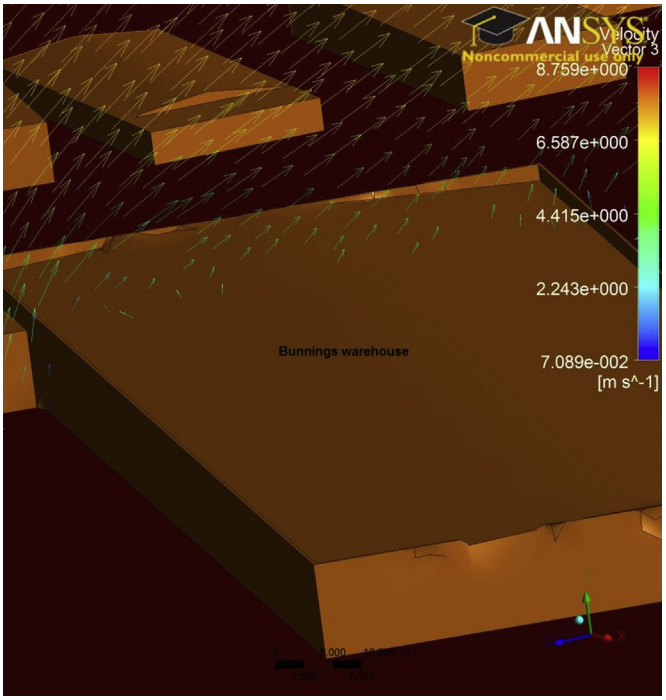

Fig. 8. Effect of the sloping angle of the rooftop of the Bunnings warehouse on the speed-up of flow over the building.

environment. The tool was used to investigate wind speed and direction on the rooftop of a building and identify the optimal location for installing the turbine taking into account zones of wind acceleration, recirculation and blockage. A CFD model of the Bunnings warehouse at Port Kennedy in Western Australia was created by means of the ANSYS CFX 14 package and the buildings around the warehouse up to a radius of 200 m were incorporated in the model geometry. The wind atlas software, WAsP, was used to predict the wind velocity at the inlet of CFD domain. Observations for WAsP were taken from a meteorological mast located 18 km from the Bunnings warehouse. The wind atlas resulting from the WAsP simulation was analysed to find the mean wind speed at each of eight wind direction sectors at 200 m a.g.l. and the mean wind speed for each sector was used to create a wind speed profile that was used as inlet flow to the CFD model. A wind monitoring system installed on the roof of the Bunnings warehouse at Port Kennedy was used to collect data for the CFD model validation. For model validation, the wind measurements above the Bunnings rooftop were filtered to select only neutrally stable wind data. To check the accuracy of the combination of CFD and wind atlas software for rooftop wind resource assessment, the 10-minute averaged mean velocity vectors from the simulations were compared with measured data.

The results of the study shows CFX provides reasonable accuracy for simulating flow around a rectangular obstacle and the combination of a CFD package with a wind atlas software such as WAsP provides a promising tool for wind resource assessments for small wind turbines on the roof of buildings. CFX predicts neutrally stable flows over the building well but further research is needed to understand how CFX results can be adjusted to predict flows across the whole range of atmospheric conditions. Having said that, it is likely that there are neutral atmospheric conditions for most of the time when power is being generated by the turbine on the roof, and so the combination of CFX with WAsP provides an applicable tool for wind resource assessment in terms of small wind turbines on rooftops.

The scope of this study was limited to wind speed and direction results. Further studies of turbulence intensity prediction on the roof are planned. In this case, modelling using CFX/WAsP as well as an inflow turbulence simulator such as TurbSim could be used. Accurate prediction of the turbulence intensity on the rooftop is very important for the application of small wind turbines in the built environment, because turbulence intensity is linked to fatigue on the machine, and is mentioned as a basic parameter to characterise turbulence in the IEC61400-2 standard on the design requirements for small wind turbines.

References

[1] Carpman N. Turbulence intensity in complex environments and its influence on small wind turbines. M.Sc. Dissertation. Department of Earth Sciences, Uppsala University; 2011.
[2] Ledo L, Kosasih PB, Cooper P. Roof mounting site analysis for micro-wind turbines. Renew Energy 2011;36:1379–91.
[3] Ayhan D, Sağlam Ş. A technical review of building-mounted wind power systems and a sample simulation model. Renew Sustain Energy Rev 2012;16:1040–9.
[4] Balduzzi F, Bianchini A, Ferrari L. Microeolic turbines in the built environment: influence of the installation site on the potential energy yield. Renew Energy 2012;45:163–74.
[5] Stankovic S, Campbell N, Harries A. Urban wind energy. Earthscan; 2009.
[6] http://en.wikipedia.org/wiki/Wind_turbine, [accessed 15.04.13].
[7] http://www.bergey.com/technical/warwick-trials-of-building-mounted-wind-turbines.
[8] http://www.cyclopicenergy.com/news/20100812-TurbineFailureHobart/Hobart-Marine-Board-Turbines.shtml.
[9] Balduzzi F, Bianchini A, Carnevale EA, Ferrari L, Magnani S. Feasibility analysis of a Darrieus vertical-axis wind turbine installation in the rooftop of a building. Appl Energy 2012;97:921–9.
[10] Makkawi A, Celik AN, Muneer T. Evaluation of micro-wind turbine aerodynamics: wind speed sampling interval and its spatial variation. Build Serv Eng Res Technol 2009;30:7–14.
[11] IEC 61400-2. Wind turbines–part 2: design requirements for small wind turbines-Annex M. 3rd ed. Geneva, Switzerland: International Electrotechnical Commission; 2011.
[12] Kalmikov A, Dupont G, Dykes K, Chan C. Wind power resource assessment in complex urban environments: MIT campus case-study using CFD analysis. In: AWEA 2010 WINDPOWER Conference. Dallas, USA; 2010.
[13] Heath MA, Walshe JD. Estimating the potential yield of small building-mounted wind turbines. Wind Energy 2010;10:271–87.
[14] Mertens S, Kuik GV, Bussel GV. Performance of an H-Darrieus in the skewed flow on a roof. Solar Energy Eng 2003;125:433–40.
[15] Mertens S. The energy yield of roof mounted wind turbines. Wind Eng 2003;6:507–17.
[16] http://www.ansys.com/Products/Simulation+Technology/Fluid+Dynamics/Fluid+Dynamics+Products/ANSYS+CFX.
[17] http://www.wasp.dk.
[18] http://www.ieawind.org/task_27_home_page.html.
[19] Golder D. Relations among stability parameters in the surface layer. Bound Layer Meteorol 1972;3:47–58.
[20] Troen I, Petersen EL. European wind atlas. Roskilde, Denmark: RisØ National Laboratory; 1989.
[21] Hossain MS. Investigating whether the turbulence model from existing small wind turbine standards is valid for rooftop sites. M.Sc. Dissertation. Perth: School of Engineering and Energy, Murdoch University; 2012.
[22] Takahashi S, Hamada J, Takashi YK. Numerical and experimental studies of airfoils suitable for vertical axis wind turbines and an application of wind-energy collecting structure for higher performance. Wind Eng 2006;108:327–30.
[23] Uchida T, Ohya Y. Micro-siting technique for wind turbine generators by using large-eddy simulation. Wind Eng Ind Aerodyn 2008;96:2121–38.
[24] Tutar M, Oguz G. Computational modelling of wind flow around a group of buildings. Comput Fluid Dyn 2004;18:651–70.
[25] Menter FR. Two-equation eddy-viscosity turbulence models for engineering applications. AIAA J 1994;32:1598–605.
[26] Sørensen NN. General purpose flow solver applied to flow over hills. PhD thesis. Lyngby: Risø-DTU; 1995.
[27] Michelsen JA. Basis3D – a platform for development of multi-block PDE solvers. Technical Report AFM 92-05. Lyngby: Technical University of Denmark; 1992.
[28] ANSYS CFX-Solver theory guide release 14.5. ANSYS, Inc.; 2012.
[29] http://www.mi.uni-hamburg.de/Introducti.433.0.html.
[30] Oberkampf WL, Roy CJ. Verification and validation in scientific computing. New York: Cambridge University Press; 2010.
[31] Oberkampf WL, Barone MF. Measures of agreement between computation and experiment: validation metrics. Computat Phys 2006;217:5–36.

[32] VDI. Environmental meteorology-prognostic micro scale wind field models – evaluation for flow around Buildings and Obstacles, VDI Guideline 3783 – part 9. Berlin: Beuth Verlag; 2005.
[33] Schluunzen KH, Hinneburg D, Knoth O, Lambrecht M, Leitl B, Lopez S, et al. Flow and transport in the obstacle layer-first results of the micro-scale model MITRAS. Atmos Chem 2003;44:113–30.
[34] Franke J. Application of Richardson extrapolation to the prediction of the flow field around building models. In: Proceedings of the 4th International Symposium on Computational Wind Engineering (CWE2006), Yokohama, Japan 2006.
[35] Eichhorn J, Kniffka A. The numerical flow model MISKAM: state of development and evaluation of the basic version. Meteorologische Zeitschrift 2010;19:81–90.
[36] VDI. Environmental meteorology-physical modelling of flow and dispersion processes in the atmospheric boundary layer – application of wind tunnels, VDI guideline 3783 – part 12. Berlin: Beuth Verlag; 2000.
[37] Franke J, Strum M, Kalmbach C. Validation of Open FOAM 1.6.x with the German VDI guideline for obstacle resolving micro-scale models. Wind Eng Ind Aerodyn 2012;104–106:350–9.
[38] Lyons TJ, Scott WD. Principles of air pollution meteorology. London: Belhaven Press; 1990.